Journal of Thoracic Imaging
8(4):249–264 © 1993 Raven Press Ltd, New York

Computed Tomography Assessment of Ground-Glass Opacity: Semiology and Significance

Martine Remy-Jardin, M.D., Jacques Remy, M.D., Frédéric Giraud, M.D., Lionel Wattinne, M.D., and Bernard Gosselin, M.D.

Se usa HRCT, nosotros queremos enfocarlo en imágenes standar (baja resolución)

Summary: Among the computed tomography (CT) signs of parenchymal lung disease, the ground-glass pattern is the one most difficult to diagnose and most influenced by CT technique. Ground-glass opacity may result from changes in the airspaces or interstitial tissues in acute or chronic infiltrative lung disease. It may also be seen as a consequence of increased capillary blood volume in redistribution of blood flow due to airway disease, emphysema, or pulmonary thromboembolism. Definition of this sign on high-resolution CT (HRCT) images, its various HRCT patterns, and potential pitfalls in its recognition are described with special attention to optimal HRCT technique. **Key Words:** High-resolution computed tomography—Ground-glass opacity.

High-resolution computed tomography (HRCT) has provided considerable improvement in the evaluation of lung parenchyma, with remarkably detailed images of lung architecture without superimposition of structures, thus enabling assessment of fine parenchymal detail (1–3). The advantages of HRCT and careful HRCT–pathology correlations have allowed the clarification of roentgenographic patterns of parenchymal involvement previously reported as "inconsistent," "misleading," and "equivocal" in the conventional radiologic literature (4).

The role of HRCT in clarifying semantic problems is nowhere better exemplified than in the recognition and interpretation of ground-glass opacity. By providing an appropriate description for this radiographic pattern, HRCT has helped transform a "nonspecific radiologic descriptor of limited usefulness" (5) on the chest radiograph into one of the most exciting signs of lung involvement. In this review, criteria for accurate CT recognition of ground-glass opacity are discussed with special emphasis on factors influencing lung density analysis on CT studies and description of potential pitfalls in recognition of this CT sign.

From the Department of Radiology (M.R.-J., J.R., F.G., L.W.), and Department of Pathology (B.G.), Hôpital Calmette, University of Lille, Lille, France.

Address correspondence and reprint requests to Dr. M. Remy-Jardin, Department of Radiology, Hôpital Calmette, Boulevard Jules Leclerc 59037, Lille Cedex, France.

DEFINITION

From initial descriptions on chest radiographs, ground-glass appearance has always been associated with the detection of an increase in lung density without obscuration of surrounding anatomic details. The main difficulty was the subjectiveness of the assessment of a radiographic sign characterized by a "fancied resemblance to etched or abraded glass" (5). The ability of CT images to yield information on tissue density introduced a new field of investigation with more precise analysis of lung density in addition to morphologic evaluation of lung changes. However, in marked contrast to precise descriptions of most of the basic CT signs of parenchymal involvement, ground-glass opacity has received far less attention. In a review of the radiologic literature on ground-glass opacity, consensus was reached on two descriptive terms: hazy increased lung density and without blurring of normal markings (2,3,6). The main discrepancy con-

cerned the shape of areas of ground-glass attenuation. Most authors fail to precisely define the shape of the areas; a few retain the term "fine granular appearance" from former descriptions of ground-glass opacities on chest radiographs (5). Providing that abnormal lung density is evaluated using optimal HRCT technique, any area of increased attenuation of "granular" appearance should be considered a nodular pattern and not a ground-glass pattern.

Ground-glass pattern can be defined by four main criteria: (a) areas of hazy and amorphous increased lung attenuation; (b) no obscuration of the underlying vascular markings and bronchial walls; (c) identification on HRCT sections; and (d) photographed with wide window settings (Fig. 1). The requirements for performing HRCT include a current technology scanner, thin slices (1–2 mm), and reconstruction using a high-spatial-frequency algorithm (7). The scans are performed during breath-holding at end-inspiration, and images are reconstructed using a matrix of 512 pixels with a 35–40-cm field of view; when necessary, a smaller field of view (12–24 cm) is used to further improve spatial resolution. The importance of technical factors in the definition of ground-glass opacity is further emphasized throughout this review.

FIG. 1. Target reconstruction of a 1-mm HRCT section through the right upper lobe in a patient with documented COPD. The section shows characteristic features of ground-glass opacity with increased lung density within which normal anatomic structures can still be visualized. Note inhomogeneous hazy increased lung density with sparing of scattered areas.

Recognition of ground-glass opacity remains based on a subjective, qualitative assessment of attenuation by an experienced radiologist. Since attenuation in the lung is very closely related to density, CT should theoretically provide an objective quantitation of ground-glass appearance. If this quantitative analysis could be relied on with a reasonable degree of certainty, objective confirmation of a visual impression could be achieved using attenuation gradients. In practice, this does not occur, since many parameters are known to interfere with lung density and to make attenuation measurements unreliable.

ASSESSMENT OF LUNG DENSITY

The attenuation coefficient for a CT lung scan is a blended value that results from the complex interplay between tissues with highly differing densities including the airways and alveoli, soft tissues (bronchi, vessels, blood, and interstitium), and interstitial fluid. CT lung density measurements are also markedly influenced by physiologic patient-related and machine-related factors.

The two most important physiologic patient-related parameters influencing lung density are the amount of air in the lung and the blood volume. The effect of posture on lung density can be understood in the context of regional differences of pulmonary perfusion and ventilation. Density gradients, primarily related to the influence of gravity, are normally present between anterior nondependent and posterior dependent portions of the parenchyma when the patient is scanned supine. These gradients result from the effects of gravity, leading to an increased amount of blood flow in the dependent lung due to gravity but also to a relatively airless lung parenchyma in the posterior lung due to the increasing weight of the lung toward the most dependent regions (8–10). When breathing takes place at low lung volume, these differences are exaggerated, including the effects of closing volume—i.e., the lung

volume at which the dependent lung zones cease to ventilate (11). Additional gradients are measurable between cortical and medullary lung. On patients scanned supine, Genereux observed anterior and posterior corticomedullary gradients in the transverse plane, which resulted from the combined effects of gravity on ventilation and perfusion (12). In healthy adult volunteers, a stratified distribution of perfusion in the horizontal plane of lungs independent of the effects of gravity was observed 10 times greater in the central region of lung compared with the lung periphery (13,14). Despite the absence of precise anatomic demarcation between the pulmonary cortex and the medulla, there is a consensus on their physiological differences; it has been suggested that physiological differences between cortex and medulla, such as blood flow regulation, could be evaluated (15). These differences are known to be considerably influenced by lung volumes. Although it has been suggested that this problem may be solved by spirometrically controlled scanning, this technique is not routinely used (16).

Problems are also encountered with the use of CT attenuation numbers (17–20). Absolute density measurements vary widely when the same phantom is scanned on different machines, with significant fluctuations resulting from variations in kilovoltage, orientation, and positioning of the patient within scanners and the size of lesions or structures to be examined (21). Significant differences in absolute CT numbers may also be seen between two scanners of the same manufacturer and model (21). Moreover, the CT technique used for parenchymal analysis may also influence recognition of abnormal lung density; this fact has been recently underlined by Zwirewich et al., who observed that low-dose HRCT technique failed to identify ground-glass opacities that were evident but subtle on the high-dose scans (22).

PITFALLS IN GROUND-GLASS PATTERN RECOGNITION

A false interpretation of ground-glass appearance may result from inadequate CT technique, incorrect interpretation of HRCT images, and/or physiologic variations.

Pitfalls related to technique

A ground-glass pattern is a CT sign that can only be confidently diagnosed on HRCT images. Although abnormal lung density can be suspected on 5–10-mm collimation scans, only thin sections (1–2 mm) allow distinction of ground-glass opacity from haziness due to volume averaging of fine parenchymal abnormalities such as linear or micronodular opacities (Fig. 2). Optimal assessment of ground-glass opacities also requires use of a large window width (range, 1,500–2,000 HU) and a high window level (range, −500 to −700 HU) for analysis of the lung parenchyma on HRCT images (23). The radiologist should be aware of the influence of window settings on the appearance of pulmonary structures. By reducing window level and width, higher contrast is achieved with subsequent magnification of vascular sections, bronchial walls (whether normal or not), and fissural thickening. The preferential magnification of small structures that is observed when using low window settings can create a pseudo–ground-glass appearance that may lead the unwary observer to overdiagnose abnormal lung density.

Pitfalls related to interpretation

Micronodular pattern

Poorly marginated, small, rounded opacities are readily recognized on cross-sectional images and should be differentiated from ground-glass opacities by their nodular shape. Nevertheless, the distinction between diffusely distributed micronodules with poor margination and ground-glass opacity may sometimes be difficult. However, this distinction is useful in the differential diagnosis of chronic infiltrative lung disease on HRCT because a fine micronodular pattern with ill-defined margins may help suggest a bronchiolar or peribronchiolar process and/or subacinar micronodules (Fig. 2).

Airspace consolidation

Airspace consolidation is characterized by increased lung density with obscuration of the surrounding vascular markings and the presence of air bronchogram. Consolidation is observed when the pulmonary parenchyma is completely or almost completely airless as a result of complete filling of the alveolar spaces with liquid, cells, or tissue or secondary to atelectasis. This pattern should be distinguished from ground-glass opacity.

Parenchymal density analysis

In cases of mild and heterogenously distributed gradients of density in the lung parenchyma, it may be difficult or impossible to distinguish a pattern of

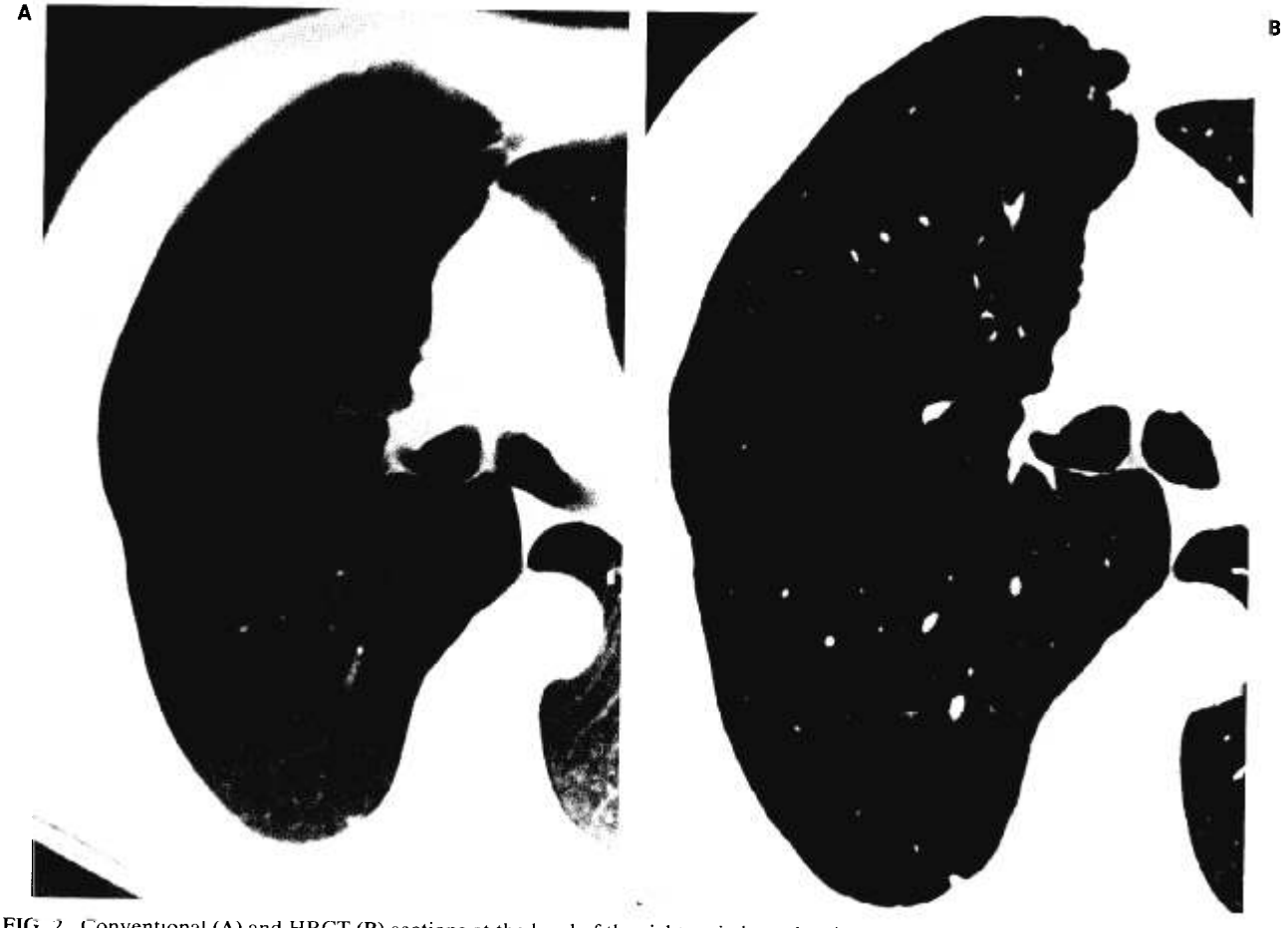

FIG. 2. Conventional (A) and HRCT (B) sections at the level of the right main bronchus in a patient with the subacute form of extrinsic allergic alveolitis (pigeon breeder's lung) are shown to demonstrate the effect of slice thickness on the analysis of parenchymal abnormalities. A 10-mm-thick section demonstrates increased lung density inhomogeneously distributed throughout the lung (A). On HRCT, the abnormal lung density does not conform to the criteria defining ground-glass pattern in that it shows a pattern of diffuse and poorly marginated micronodules, with a few having a centrilobular distribution (B).

normal lung intermingled with areas of ground-glass attenuation from a pattern of areas of abnormally low attenuation against normal lung. To provide optimal assessment, the HRCT images must be interpreted in the context of clinical history, physical data, and pulmonary function tests.

Pitfalls due to physiologic variations

Ground-glass opacity and expiratory scans

Several investigators have demonstrated an attenuation coefficient gradient, related primarily to the influence of gravity on blood flow, that is normally present between the nondependent and dependent portions of the lung in the supine, prone, and lateral decubitus positions (1,7,24,25). Zerhouni et al. observed that these anteroposterior gradients are smaller at full inspiration than at full expiration, with the inspiratory–expiratory gradient slightly higher in the left lung than in the right lung and more pronounced in the gravity-dependent portions of the posterior–inferior regions of the lower and upper lobes (24). This attenuation coefficient gradient is often undetectable on visual inspection of HRCT images obtained at full inspiration. Since a diffuse ground-glass opacity is a constant CT finding on normal scans taken at or near end-expiratory volumes, any mild parenchymal abnormality can be easily overlooked or obscured by this physiological feature; therefore, CT scans must be performed during breath-holding at end-inspiration.

Dependent ground-glass pattern

Aberle et al. demonstrated subpleural dependent density on inspiratory scans in 17% of cases of a control group. These abnormalities result from an increased amount of blood flow in dependent lung and from a gravity-dependent variation in the size

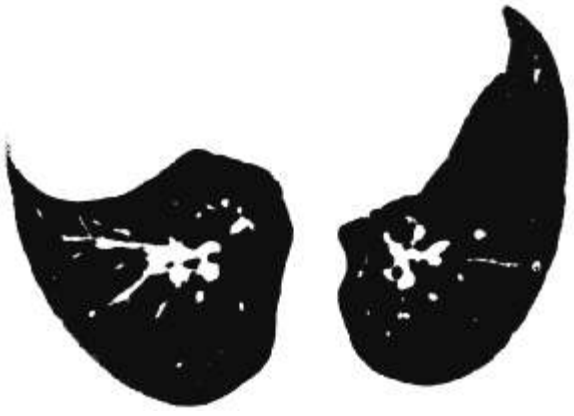

FIG. 3. HRCT section at the level of the lower lobes in a patient with idiopathic pulmonary fibrosis demonstrates a mild and homogeneous increase in lung density, diffusely distributed through both lungs. The "darker air bronchogram," observed bilaterally, is the sole CT sign suggesting ground-glass opacity.

of alveoli, which accounts for the decreased amount of air in the posterior lung (26). In a study of 175 healthy adult volunteers, Remy-Jardin and coworkers observed statistically significant differences in the frequency of dependent ground-glass opacity among smokers (current smokers, 34%; ex-smokers, 43%) compared with nonsmokers (12%), suggesting that disease of the small airways could be an additional factor responsible for hypoventilation in dependent lung zones (27). However, no correlation was found between this CT finding and abnormalities at low lung volumes on flow–volume curves.

HRCT PATTERNS OF GROUND-GLASS ATTENUATION

The recognition of ground-glass opacities on HRCT images is influenced by the intensity and the extent of the areas of increased lung density. Areas of ground-glass opacity can be easily detected when there is a marked increase in lung density and when the lung involvement is patchy in distribution (Fig. 1). Conversely, a mild increase in lung density can be easily overlooked, particularly when the ground-glass pattern is diffuse and homogeneous throughout the lungs. Presence of the sign described by Naidich et al. as the "darker air bronchogram" may serve as a marker of ground-glass opacity (Fig. 3) (6).

A variety of zonal patterns of distribution of ground-glass opacities within the lung have been documented, although they do not represent distinguishing features suggesting specific etiologies per se. The most frequent finding is the multifocal or diffuse ground-glass pattern, characterized by patchy, more or less coalescent areas of increased attenuation (Fig. 6). When the gradient of density between normal and abnormal lung is high, recognition of multifocal ground-glass pattern is easily done by visual analysis. In the presence of a low gradient density, recognition of ground-glass pattern may be helped by using narrow windows to intensify mild density differences. Occasionally, ground-glass opacity may assume a lobar or segmental distribution. Geographic distribution in which there is a sharp line of demarcation between normal and abnormal lung can be observed, allowing identification of cortical or medullary patterns (Fig. 5). The lobular distribution of ground-glass opacity can be readily appreciated on cross-sectional images when areas of increased attenuation are sharply marginated by interlobular septa.

Ground-glass opacities may be observed as isolated CT findings or combined with other patterns of lung disease. The most frequent associations are with micronodular patterns or cystic airspaces. A micronodular pattern is easily discerned when seen superimposed on a diffuse background of ground-glass opacity. Abnormal lung density does not interfere with interpretation of honeycombing. Nevertheless, when areas of low attenuation secondary to emphysematous changes are outlined by ground-glass opacity, definable "walls" of various thicknesses around emphysematous lesions, responsible for a network of lattice elements resembling the typical honeycomb pattern, may be seen. When observed in the dependent regions of the lungs, pseudohoneycombing is easily distinguished by comparing prone and supine sections obtained at the same level, which should demonstrate reversal of both dependent ground-glass opacities and the "walls" of cystic air spaces (Fig. 6). The size of vessels is an important semiologic feature in the analysis of HRCT images; the presence of increased pulmonary and/or venous sections through areas of ground-glass pattern is a hallmark of the hemodynamic ground-glass pattern.

SIGNIFICANCE OF GROUND-GLASS PATTERN

Because lung density results from the relative proportions of blood, gas, extravascular water, and pulmonary tissue, increased lung density may result from changes in the airspaces or the extravascular

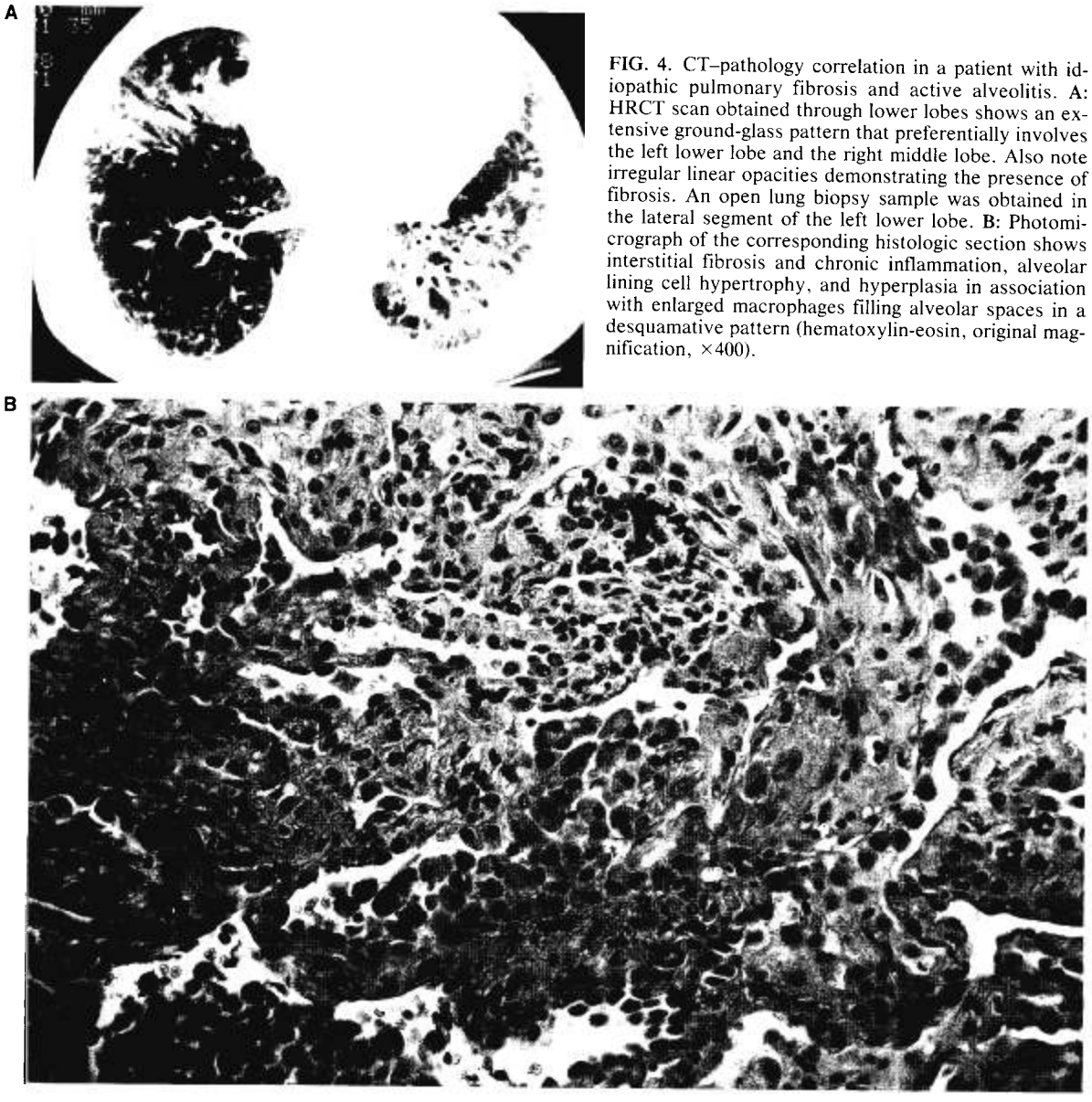

FIG. 4. CT–pathology correlation in a patient with idiopathic pulmonary fibrosis and active alveolitis. A: HRCT scan obtained through lower lobes shows an extensive ground-glass pattern that preferentially involves the left lower lobe and the right middle lobe. Also note irregular linear opacities demonstrating the presence of fibrosis. An open lung biopsy sample was obtained in the lateral segment of the left lower lobe. B: Photomicrograph of the corresponding histologic section shows interstitial fibrosis and chronic inflammation, alveolar lining cell hypertrophy, and hyperplasia in association with enlarged macrophages filling alveolar spaces in a desquamative pattern (hematoxylin-eosin, original magnification, ×400).

interstitial tissue [as in diffuse infiltrative lung disease (DILD)] or from an increase in capillary blood volume.

Ground-glass pattern in chronic DILDs

The infiltrative lung diseases are a heterogenous group of disorders of varied etiologies sharing similar histological features. These diseases usually involve the lung, in a multifocal rather than diffuse manner, beginning with an accumulation of inflammatory cells in the alveolar septa and airspaces and often culminating in severe fibrosis of the interstitium, the supporting structure of the lung (28). Although the ground-glass pattern is not a specific sign of DILD, there is considerable interest in demonstrating its presence on HRCT images in patients with suspected or known DILD because it often reflects mild parenchymal alterations, unsuspected on the radiographs, and it may provide information about disease activity and prognosis.

Pathologic basis for ground-glass appearance

The best known significance of ground-glass opacity is to reflect an active inflammatory process, representing the acute phase of lung injury often referred to as alveolitis. During this phase, two

FIG. 5. Target reconstruction of a 1-mm-thick HRCT section at the level of the right upper lobe bronchus in a patient with pulmonary hemorrhage secondary to Goodpasture syndrome shows an exclusive distribution of ground-glass opacity in the medullary portion of the lung with sharp delineation between areas of normal and abnormal lung.

main pathologic features are observed, involving both the interstitium and the airspaces in the majority of chronic interstitial lung diseases: abnormal thickening of the alveolar wall interstitium and incomplete filling of the alveolar spaces with inflammatory cells, cellular debris, and edema. Changes occurring during this phase of lung injury reduce the amount of air in affected areas without any architectural destruction, thus resulting in areas of increased lung density or "ground-glass pattern" (Fig. 4). This CT pattern may sometimes reflect isolated mural inflammation without airspace filling (Fig. 7).

Ground-glass opacity may also result from the chronic changes that are known to occur following the acute phase of lung injury in the absence of complete healing corresponding to lung fibrosis with or without lung distortion (Fig. 8). This CT interpretation is based on knowledge of pathologic changes observed during the chronic forms of DILD (6,28–30). The fibroblastic reaction associated with residual alveolar infiltrates and debris leads to reduction of the amount of air; by similar mechanisms as previously described in the acute phase of lung injury, these changes can be responsible for ground-glass opacity. In the latest stages of lung response to injury, alveolar structure is destroyed and the interstitium is no longer recognizable as a distinct entity. Healing by fibrosis leads to formation of dense areas of collagen interspersed with regions of parenchymal destruction; the resultant cystic and destructive changes constitute the hallmarks of late-phase lung disease. When cystic changes are within the resolution capabilities of HRCT, a classic honeycomb pattern appears in which cystic airspaces and traction bronchiectasis are identified. When cystic changes are too small to be detected by thin HRCT images, volume averaging of the tiny parenchymal cysts that characterize the microcystic honeycomb pattern may lead to ground-glass opacity. Bronchi in areas of lung distortion appear dilated and deformed secondary to this underlying destructive process, which involves the peribronchial connective tissue sheaths (30).

The presence of so-called traction bronchiectasis and bronchiolectasis is a reliable indirect sign of lung destruction on CT images even in the absence of typical honeycombing. In the absence of open lung biopsy and subsequent CT–pathology correlation, the only possibility that allows the radiologist to assess lung fibrosis is to identify traction bronchiectasis and/or bronchiolectasis within areas of ground-glass attenuation, a direct result of the fibrotic process (Fig. 9).

Clinical impact

Ground-glass opacity, as an isolated CT finding or in association with other parenchymal abnormalities, has been reported in various chronic DILDs (CDILDs), including alveolar proteinosis, sarcoidosis, fibrosing alveolitis, bronchiolitis, obliterans with organizing pneumonia (BOOP), chronic eosinophilic pneumonia, and radiation pneumonitis. Grenier et al. demonstrated that ground-glass opacity was among the discriminant radiographic and CT findings for the correct diagnosis in five groups of CDILDs, including sarcoidosis, idiopathic pulmonary fibrosis, histiocytosis X, silicosis, and a fifth group composed of miscellaneous diseases (31). However, ground-glass appearance had only a moderate discriminant value in differentiating among

FIG. 6. Target reconstructions of a 1-mm HRCT scan in the supine (A) and prone (B) positions at the level of the right lower lobe bronchus in a patient with COPD and extensive emphysema. Areas of low attenuation with definable "walls" are seen (A), suggesting a reticular lattice of parenchymal cysts through areas of mild ground-glass opacity in the dependent lung. This reconstruction (B) shows reversal of ground-glass opacity and subsequent disappearance of previously definable "walls" around areas of low attenuation, now characteristic of emphysematous lesions. Note small septal lines in the posterior subpleural region.

the five groups when considering radiographic and CT findings ranked by stepwise discriminant analysis.

The most important clinical application of ground-glass identification in CDILD is the assessment of disease activity. Evaluating the cellularity and degree of fibrosis of the pulmonary parenchyma pathologically is the foundation on which the prognosis and response to treatment are based. The cellular alveolar reaction is not only the earliest finding in many DILDs but it is also the "active" inflammatory lesion. Information about the presence of alveolitis helps stage disease activity and predict the likelihood of reversal of functional impairment and response to therapy. A patient with extensive interstitial lung disease composed of active alveolitis and mild fibrosis has a better chance of benefitting from therapy than a patient with a similar radiographic extent of disease composed of extensive fibrosis and little residual alveolitis.

Open lung biopsy is an invasive procedure not routinely indicated in DILDs. In most cases, a noninvasive approach is used to evaluate disease activity, such as bronchoalveolar lavage (BAL), gallium scanning, and/or CT scanning (32–34). Although gallium scanning is of limited use in fibrosing alveolitis, BAL has been reported to be useful in characterizing this finding. However, discrepancies between BAL results and open lung biopsies suggest that the cellular sampling obtained by BAL does not systematically reveal what happens in the alveolar spaces but may reflect the inflammatory reaction occurring in the bronchiolar and peribronchiolar areas (35). In patients with interstitial lung disease of unknown etiology, there are insufficient data to suggest that BAL provides information that can be

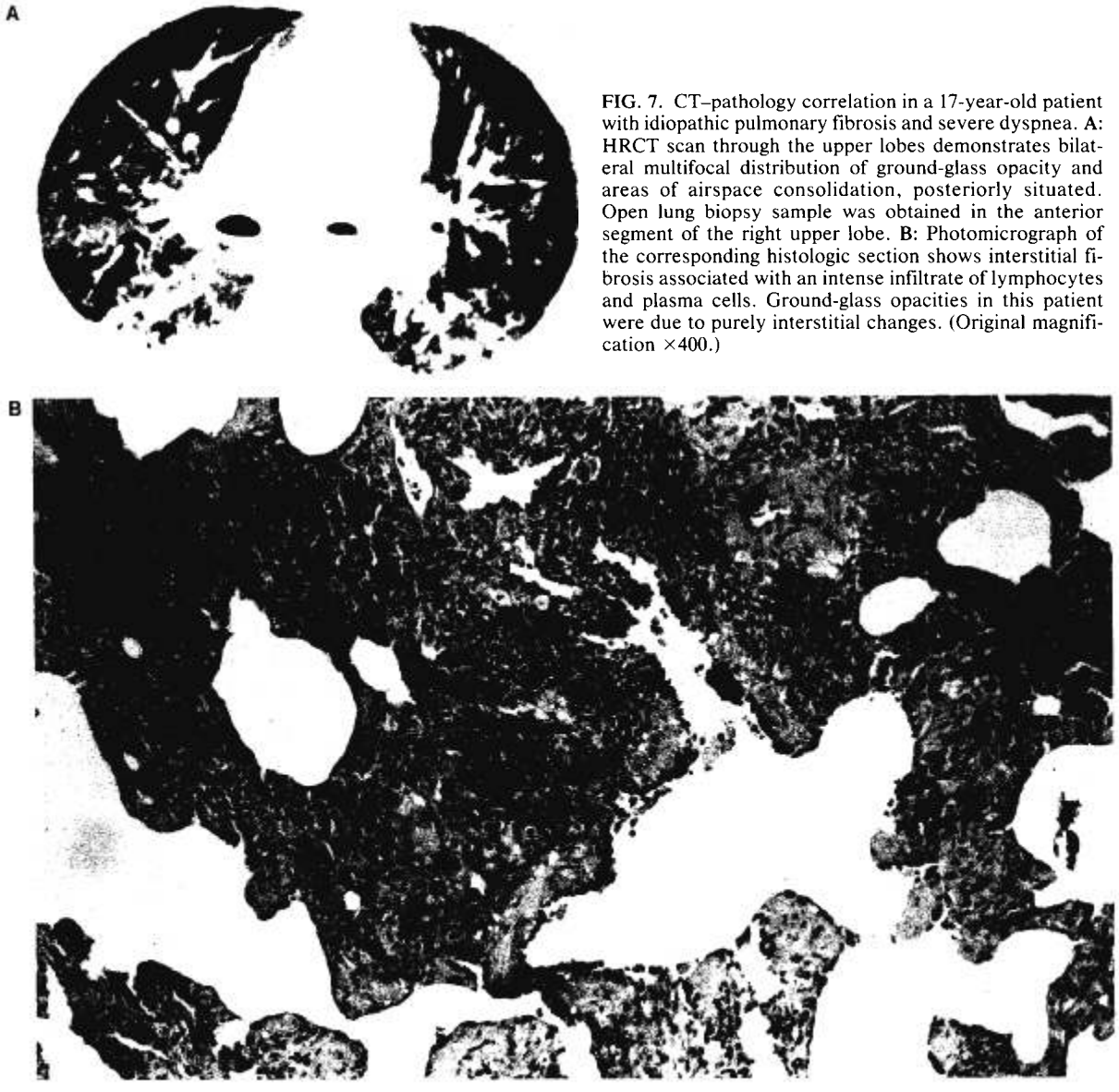

FIG. 7. CT–pathology correlation in a 17-year-old patient with idiopathic pulmonary fibrosis and severe dyspnea. A: HRCT scan through the upper lobes demonstrates bilateral multifocal distribution of ground-glass opacity and areas of airspace consolidation, posteriorly situated. Open lung biopsy sample was obtained in the anterior segment of the right upper lobe. B: Photomicrograph of the corresponding histologic section shows interstitial fibrosis associated with an intense infiltrate of lymphocytes and plasma cells. Ground-glass opacities in this patient were due to purely interstitial changes. (Original magnification ×400.)

used to determine the need for therapy, to predict response to therapy, and to determine when therapy can be discontinued (36).

Since disease activity is reflected by interstitial and intraalveolar cellularity, it was postulated that such activity might result in opacification of airspaces on CT scans and that the degree of increased density compared with the surrounding parenchyma might indicate the degree of inflammatory disease activity (37). The role of CT as predictor of disease activity has been reported mainly with fibrosing alveolitis and sarcoidosis (37–41). Müller et al. demonstrated among patients with fibrosing alveolitis that when there was marked disease activity seen pathologically, there was patchy, predominantly peripheral, opacification of airspaces; all patients evaluated by HRCT with marked or mild disease activity pathologically were correctly categorized by these observers (38). Hansell et al. confirmed the capacity of HRCT to distinguish irreversible fibrosis from acute alveolitis in most patients with fibrosing alveolitis (42). In sarcoidosis, the pathologic correlate of focal increase in lung density on HRCT is not clear, possibly due to widespread interstitial granulomata of a size below the limits of resolution of the HRCT technique or to interstitial and alveolar inflammation (39,41).

Because ground-glass opacity may also reflect

FIG. 8. CT–pathology correlation in a patient with idiopathic pulmonary fibrosis. **A:** HRCT scan obtained in prone position through lower lobes shows diffuse and uniform ground-glass opacity associated with a few ill-defined micronodules. Note the darker air bronchogram sign. Open lung biopsy sample was obtained in the posterior segment of the left lower lobe. **B:** Photomicrograph of the corresponding histologic section demonstrates parenchymal collapse in association with intense smooth muscle proliferation and cellular infiltration by multinucleate giant cells with cholesterol deposits and numerous macrophages. (Original magnification ×400.)

the presence of extensive parenchymal fibrosis with minimal alveolitis, this sign has limited specificity (43). Further studies are required to determine the precise role of HRCT in the assessment of disease activity. As CT accurately reflects the changes seen macroscopically on the lung specimen, identification of areas of ground-glass opacity is potentially useful in guiding the surgeon to the best biopsy site.

Retrospective assessment of disease activity remains possible on follow-up CT scans when decrease or complete resolution of ground-glass opacity is observed spontaneously or after treatment (Fig. 10) (39,44). Conversely, stability of ground-glass opacity after steroid treatment allows retrospective assessment of fibrosis. When follow-up CT scans demonstrate sequential replacement of ground-glass opacity by typical honeycombing, the initial CT finding may correspond to pathologic changes observed in the acute phase of lung injury or it may be due to partial volume averaging with thickened interstitial tissue or a microcystic honeycomb pattern on HRCT images.

Ground-glass pattern in acute lung infiltration

Ground-glass opacity may be observed in all situations characterized by acute lung infiltration in

acutely or subacutely ill patients. This CT sign is thus considered to represent mild to moderate alveolar filling, preceding the stage of completely airless alveoli that leads to airspace consolidation. HRCT can detect a ground-glass pattern (i.e., airspace processes) before it becomes apparent on plain films, providing extra time over eventual detection by plain films and accurately pinpointing abnormal areas for eventual bronchoscopic sampling.

In immunocompromised patients, various infectious processes may cause increased lung density from mild ground-glass pattern to dense consolidation according to the level of lung infiltration. A common cause of pulmonary infection in the immunocompromised host is *Pneumocystis carinii* pneumonia (PCP). Bergin et al. reported that ground-glass opacity was a constant but nonisolated CT finding in PCP, uniformly distributed or observed with a mosaic pattern involving some secondary lobules and sparing others (45). Results of transbronchial biopsies suggested that the ground-glass opacity in the infected lungs was caused by an inhomogeneous combination of thickened alveolar walls and foamy exudates, which fill alveoli in a multifocal distribution. This CT appearance in immunocompromised patients is suggestive of PCP but not specific of this entity, and it is not surprising to observe this sign in cases of early pneumonia caused by a variety of organisms (46). Nevertheless, the greater sensitivity of CT than chest radiography in detecting parenchymal changes at a time when the patient has significant respiratory dysfunction and a normal chest radiograph may lead to consideration of CT as an effective monitoring tool to guide diagnostic and therapeutic decisions. In severely immunocompromised patients, ground-glass opacity surrounding a central dense nodular infiltrate, referred to as the "halo" sign, may help to suggest the diagnosis of invasive aspergillosis (47).

Pulmonary hemorrhage may also be a cause of

FIG. 9. HRCT scan obtained at the level of the lower lobes shows extensive areas of ground-glass opacity associated with peripheral micronodules. Note dilated bronchi within areas of increased lung density; the interpretation was traction bronchiectasis within areas of lung fibrosis.

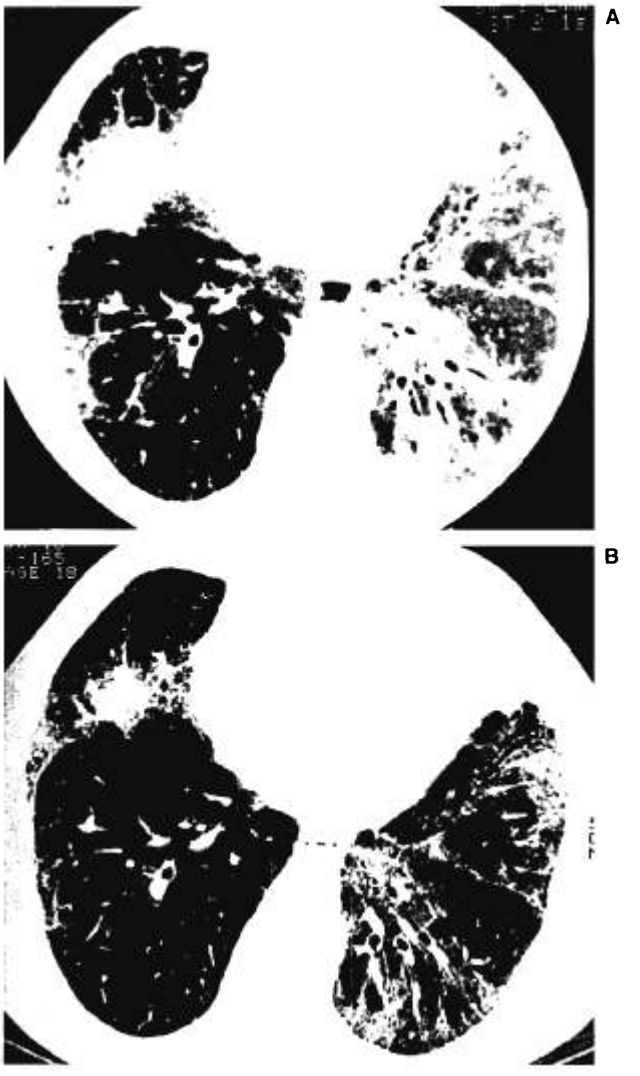

FIG. 10. Initial and follow-up HRCT scans in a patient with idiopathic pulmonary fibrosis treated with corticosteroids. A: Extensive ground-glass opacities with marked involvement of the lingula and left lower lobe are seen with relatively mild disease elsewhere. Note additional airspace consolidation in the subpleural areas of the right middle lobe and lingula and thickening of both major fissures. B: Scan obtained 6 months later at the same level shows a dramatic although incomplete resolution of ground-glass opacity in both lungs, retrospectively demonstrating that ground-glass opacity was mainly related to reversible inflammatory lesions.

ground-glass opacity on HRCT images, it is demonstrated either clinically by means of bronchoalveolar lavage–CT correlation or experimentally (48). We observed ground-glass opacity exclusively distributed in the medulla of the lung in a patient with pulmonary hemorrhage due to Goodpasture syndrome (Fig. 4). The mechanism causing the cortex to be spared is unclear. In the early CT evaluation of patients with hemoptysis, detection of ground-glass opacity may help localize the bleeding site, which may be of value when fiberoptic bronchoscopy is noncontributory. A segmental or lobar distribution of ground-glass opacity should suggest the possibility of recent bronchoalveolar lavage, especially if it is observed in the right middle lobe.

Ground-glass pattern of hemodynamic origin

Regional alterations in pulmonary blood flow and subsequent changes in regional blood volume are common hemodynamic factors shared by various clinical situations in which ground-glass opacity can be seen on HRCT images. In most cases, adjacent areas of hyper- and hypoperfused lung have great attenuation differences, and the presence of increased vascular diameters through the abnormal lung density will help identify ground-glass opacity of hemodynamic origin.

Redistribution of blood flow in pulmonary diseases

Ground-glass opacity identified in patients with chronic obstructive pulmonary disease (COPD) may be the result of a regional increased blood flow secondary to widespread narrowing of vessel lumina in the pulmonary arterial bed due to vascular smooth muscle contraction and/or structural changes in vessel walls (49). The most important stimulus for pulmonary arterial vasoconstriction is alveolar hypoxia. Alterations in regional blood flow affect lung attenuation by increasing and decreasing blood volume in the capillary bed, a phenomenon previously described as mosaic oligemia (50). Moreover, the denser areas representing hyperperfused lung may appear with even higher contrast than the surrounding lung when destructive changes, air trapping, and oligemic changes act as cofactors responsible for areas of abnormally low attenuation. These regional differences in lung attenuation in patients with COPD or bronchiolitis are increased on expiratory scans (Fig. 11).

The extent of ground-glass opacity secondary to redistribution of blood flow varies with the extent of the underlying pulmonary process. In COPD, there

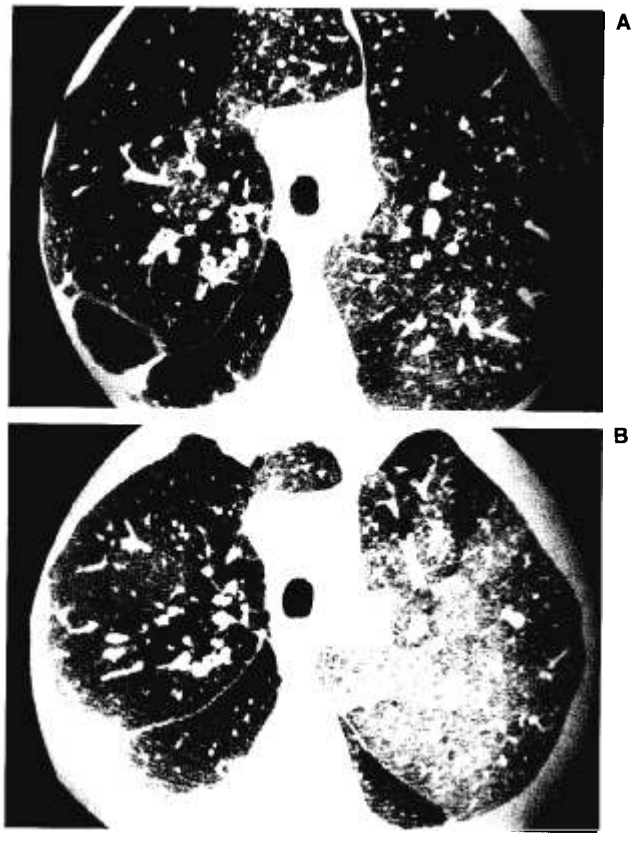

FIG. 11. Ground-glass opacity of hemodynamic origin in a patient with COPD. A: HRCT scan at end-inspiration through upper lobes shows abnormal bronchial thickening and multifocal distribution of ground-glass opacity. Note that diameters of vessels in more opaque lung are substantially larger than in the more lucent areas; the former represent hyperperfused lung due to redistribution of blood flow and the latter show more oligemic zones secondary to hypoxic vasoconstriction. B: These differences are accentuated when the scan is obtained at end-expiratory lung volume; areas of trapped air are also seen.

is often a multifocal abnormality although more limited alterations in lung density may be observed. In cases of extensive lung destruction, ground-glass opacity will be seen in the remaining, more normal lung in the parts macroscopically spared by the underlying pathology. We observed large vascular diameters in areas of ground-glass opacity exclusively distributed in the upper lung zones in patients with bibasilar destruction by panacinar emphysema; conversely, this CT pattern was exclusively distributed in the lower lung zones in a patient with extensive lung fibrosis and predominant involvement of the upper lung zones.

Chronic thromboembolic disease

To our knowledge, Martin et al. were the first authors to point out that regional alterations in pul-

monary blood flow secondary to chronic thromboembolic disease could cause increased lung density (50). In our clinical experience, ground-glass opacity in patients with chronic thromboembolic disease is often sharply demarcated with lobular borders; increased vascular sections through the abnormal lung density have been a constant feature (Fig. 12). Mosaic oligemia is the best known factor contributing to increased lung density. When branches of the arterial bed are occluded, there is a subsequent increase in blood flow in the remaining patent areas in order to maintain the cardiac output (50). There are two additional but usually transient factors that explain the regional increase in lung attenuation immediately after pulmonary arterial occlusion: edema and pulmonary hemorrhage. They are known to occur in the occluded area with subsequent resolution, except when pulmonary embolism is followed by parenchymal infarction. A third parameter potentially responsible for increased lung density in occluded areas is the development of systemic collateral supply in the occluded area that enters the pulmonary circulation, distal to the site of obstruction, angiographically observed as antegrade systemic-to-pulmonary arterial shunts (51).

Similar mechanisms to those observed after acute or chronic thromboembolism are suspected to occur in the weeks and months following embolotherapy of pulmonary arteriovenous malformations. We observed asymptomatic ground-glass opacity after occlusions of peripheral pulmonary arteriovenous malformations treated by occlusion with steel coils of distal arterial branches (51,52). Occurrence of

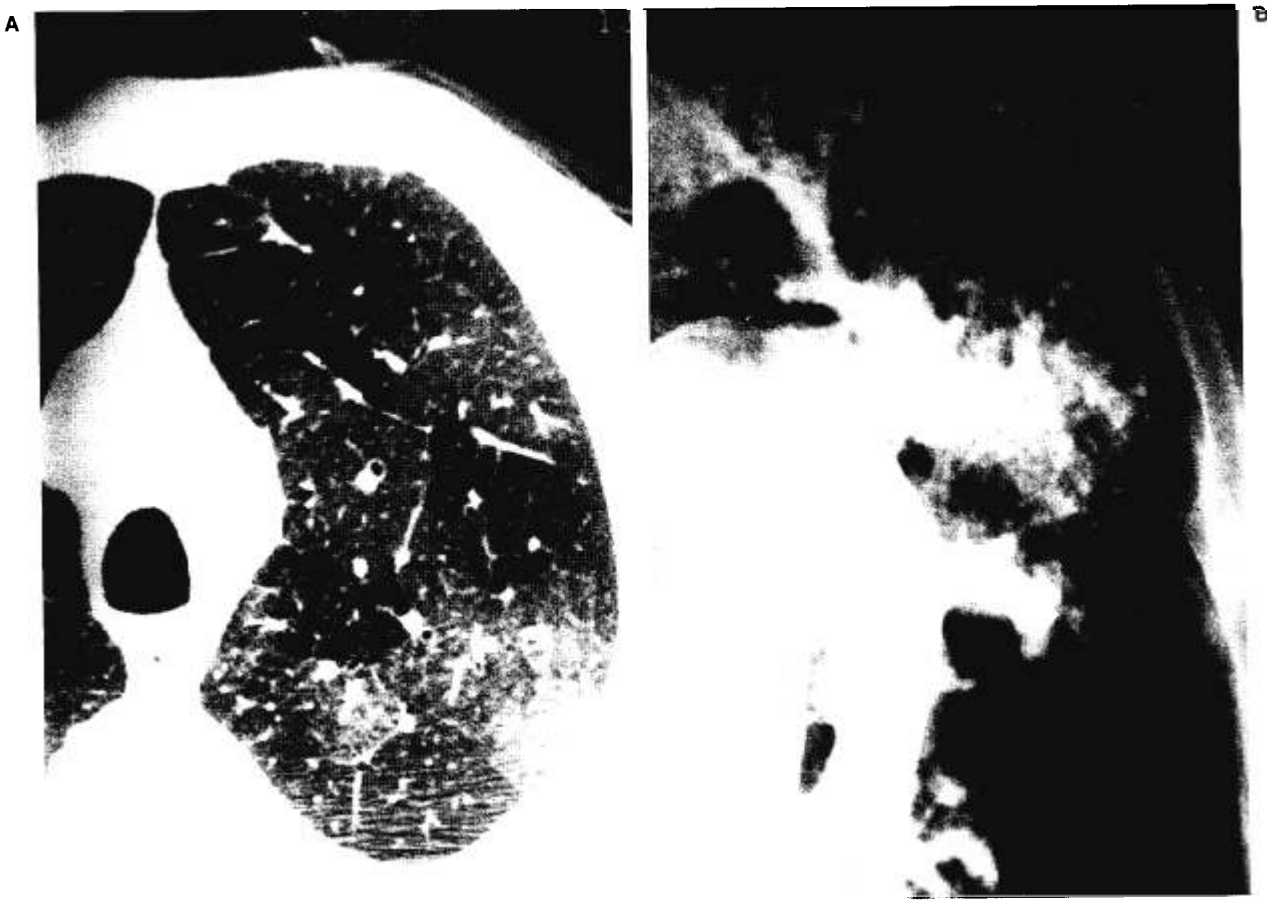

FIG. 12. Ground-glass opacity of hemodynamic origin in a patient with chronic thromboembolic disease. A: Target reconstruction of a 1-mm HRCT section at the level of the left upper lobe shows multifocal ground-glass opacity with more prominent vascular sections within areas of increased attenuation compared with normal lung, suggesting redistribution of blood flow. Note sharp lines of demarcation surrounding areas of ground-glass opacity; these are lobular borders. B: Magnified view of the left pulmonary angiogram demonstrates multiple areas of absent perfusion and zones of increased blood flow in the remaining patent pulmonary arteries of the left upper lobe, which account for the areas of ground-glass attenuation on the HRCT scan.

these transient abnormalities may suggest either edema or hemorrhage, but they may also be interpreted as a CT demonstration of hyperemia resulting from systemic supply of the occluded area.

Pulmonary hypertension

Ground-glass opacity may help suggest pulmonary hypertension, especially when associated with enlarged central pulmonary arteries (53,54). This CT pattern was observed in a patient with Osler–Weber–Rendu disease and recent-onset pulmonary hypertension of unknown etiology (52). We observed large pulmonary vascular diameters in parenchymal areas with a mild increase in attenuation that was sharply demarcated and present in both lungs, suggesting a typical ground-glass opacity secondary to redistribution of blood flow.

Pulmonary edema

Pulmonary edema of cardiac origin. Pulmonary edema is the consequence of high pulmonary capillary and venous pressure due to failure of the left side of the heart. Pulmonary edema fluid may lie in the alveolar spaces (i.e., alveolar pulmonary edema), or it may be restricted to the interstitial tissue of the lung (i.e., interstitial pulmonary edema). Grainger emphasized that identification of interstitial edema could be confidently obtained by means of adequate radiological evaluation (55). The first radiological evidence of interstitial edema on chest radiographs is the presence of Kerley's lines, mainly observed at the costophrenic angles (B lines) and less frequently observed near the hila (A lines); these lines are related to the interlobular septal thickening caused by interstitial edema and dilated lymphatics. When the surrounding alveoli become waterlogged, the typical radiographic pattern of alveolar edema occurs.

Detection of subclinical forms of pulmonary edema has been aided by the HRCT and understanding the findings on CT of the chest in experimental pulmonary edema (56–58). In patients with raised pulmonary venous pressure due to left heart failure but no auscultatory signs, CT may detect pulmonary edema by recognition of pulmonary extravascular lung water either in the interstitial tissue (i.e., interlobular septal thickening) or in the alveoli (i.e., featureless or sharply demarcated areas of ground-glass opacity); there may also be dilated vessels through the abnormal lung density due to hemodynamic changes (Fig. 13). Wegenius experimentally demonstrated the sequence of fluid accumulation in lung as quantal (i.e., all or none), with the pattern of reaction of each individual alveolus being stereotyped as either air-filled and expanded or fluid-filled and collapsed (58). As suggested, the behavior of an individual alveolus can be observed indirectly by looking at groups of alveoli, a situation clinically encountered on CT examinations. The distribution is usually bilateral and almost symmetrical, but distribution of parenchymal abnormalities must be interpreted in the context of the presence or absence of precapillary hypertension, since obstructive arterial changes are known to interfere with regional distribution of blood flow (55). Coates et al., studying the effect of a rapid infusion of normal saline on lung density in normal adult volunteers, demonstrated that an increase in lung den-

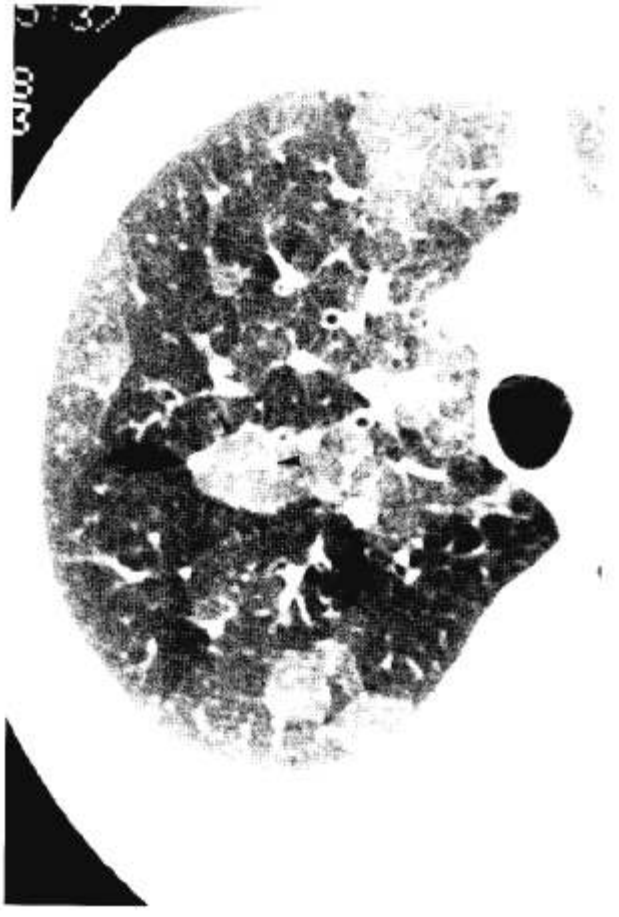

FIG. 13. Target reconstruction of a 1-mm HRCT scan at the level of the right upper lobe in a patient with pulmonary edema due to mitral disease. Note lobular distribution of ground-glass opacity marginated by interlobular septa (small arrows). The presence of a dilated centrilobular artery (arrowhead) and dilated perilobular pulmonary veins (large arrows) suggests that the ground-glass opacity reflects alveolar and/or interstitial pulmonary edema secondary to increased pulmonary venous pressure.

sity following acute expansion of the extracellular fluid volume was not detectable by conventional CT if the change was less than 15% (59). Significant reduction of ground-glass opacity after treatment of left heart failure adds to the possibility that ground-glass opacity may be due to minimal alveolar infiltration.

Other causes of pulmonary edema. Identical CT findings are expected to be found in pulmonary edema of any etiology—that is, in all situations where the capacity of the lung lymphatics to drain capillary transudate is exceeded—including venous and lymphatic obstruction, increased capillary permeability, and hypoproteinemia. We observed similar CT findings to those described with cardiogenic pulmonary edema in a case of congenital pulmonary lymphangiectasis associated with a chylous pleural effusion (60). The pathologic basis for CT interpretation can be summarized as follows: interlobular septa are thickened by interstitial edema and dilated septal lymphatics, and mild alveolar edema occurs secondary to inefficient lymphatic drainage via congenitally obstructed lymphatics either in the hilum or the mediastinum or secondary to malformations of the thoracic duct. Similar criteria are suggested for the ground-glass pattern observed on HRCT images of patients with lymphangitic carcinomatosis.

To our knowledge, no precise HRCT evaluation of the pulmonary parenchyma has been reported in patients with venoocclusive disease. Maltby and Gouverne described gravity-dependent edema with bilateral pleural effusion associated with dilated arterial sections and small-sized central pulmonary veins and left atrium on conventional CT images (61).

CONCLUSION

HRCT offers the best radiographic modality available for detecting ground-glass opacity. The level of scanner resolution and close attention to detail on HRCT images allow not only depiction of areas of increased lung density but also, in selected cases, information about the histological features of the lung parenchyma and the hemodynamic status of the pulmonary circulation. Familiarity with the interpretation of HRCT scans and the use of optimal technique are mandatory for correct evaluation of lung density changes.

REFERENCES

1. Webb WR. High resolution CT of the lung parenchyma. *Radiol Clin North Am* 1989;27:1085–97.
2. Klein J, Gamsu G. High resolution computed tomography of diffuse lung disease. *Invest Radiol* 1989;24:805–12.
3. Müller NL, Miller RR. Computed tomography of chronic diffuse infiltrative lung disease. *Am Rev Respir Dis* 1990; 142:1206–15.
4. Mathieson JR, Mayo JR, Staples C, Müller NL. Chronic diffuse infiltrative lung disease: comparison of diagnostic accuracy of CT and chest radiography. *Radiology* 1989;171: 111–6.
5. Glossary of terms for thoracic radiology: recommendations of the Nomenclature Committee of the Fleischner Society. *AJR* 1984;143:509–17.
6. Naidich DP, Zerhouni EA, Siegelman S, eds. *Computed tomography and magnetic resonance of the thorax*. 2nd ed. New York: Raven Press, 1991:341–405.
7. Mayo JR, Webb WR, Gould R, et al. High resolution CT of the lungs: an optimal approach. *Radiology* 1987;163:507–10.
8. West JB, Dollery CT, Naimark A. Distribution of blood flow in isolated lung: relation to vascular and alveolar pressures. *J Appl Physiol* 1964;19:713–24.
9. Murata K, Itoh H, Senda M, Todo G, Yonekura Y, Torizuka K. Ventilation imaging with positron emission tomography and nitrogen 13. *Radiology* 1986;158:303–7.
10. Reed JH, Wood EH. Effect of body position on vertical distribution of blood flow. *J Appl Physiol* 1970;28:303–11.
11. Leblanc P, Ruff F, Milic-Emili J. Effects of age and body position on "airway closure" in man. *J Appl Physiol* 1970; 28:448–51.
12. Genereux GP. Computed tomography of the lung: review of anatomic and densitometric features with their clinical application. *Can Assoc Radiol J* 1985;36:88–102.
13. Hakim TS, Lisbona R, Dean GW. Gravity-independent inequality in pulmonary blood flow in humans. *J Appl Physiol* 1987;63:1114–21.
14. Lisbona R, Dean GW, Hakim TS. Observation with SPECT on the normal regional distribution of pulmonary blood flow in gravity independent planes. *J Nucl Med* 1987;28:1758–62.
15. Vock P, Salzmann C. Comparison of computed tomographic lung density with haemodynamic data of the pulmonary circulation. *Clin Radiol* 1986;37:459–64.
16. Kalender WA, Rienmuller R, Seissler W, Behr J, Welke M, Heninz-Fichte D. Measurement of pulmonary parenchymal attenuation: use of spirometric gating with quantitative CT. *Radiology* 1990;175:265–8.
17. Wegener OH, Koeppe P, Oeser H. Measurement of lung density by computed tomography. *J Comput Assist Tomogr* 1978;2:263–73.
18. Hedlund LW, Anderson RF, Goulding PL, Beck JW, Effmann EL, Putman CE. Two methods for isolating the lung area of a CT scan for densitometry information. *Radiology* 1982;144:353–7.
19. Hedlung LW, Vock P, Effman EL. Evaluation of lung density by computed tomography. *Semin Respir Med* 1983;5: 76–87.
20. Rosenblum LJ, Maureci RA, Wellestein DE, et al. Density patterns in the normal lung as determined by computed tomography. *Radiology* 1980;137:409–16.
21. Levi C, Gray JE, McCullough EC, Hattery RR. The unreliability of CT numbers as absolute values. *AJR* 1982;139: 443–7.
22. Zwirewich CV, Mayo JR, Müller NL. Low-dose high-resolution CT of the lung parenchyma. *Radiology* 1991;180: 413–7.
23. Naidich DP, Zerhouni EA, Siegelman S, eds. *Computed tomography and magnetic resonance of the thorax*. 2nd ed. New York: Raven Press, 1991:1–34.
24. Zerhouni EA, Naidich DP, Stitik FP, et al. Computed tomography of the pulmonary parenchyma. II. Interstitial disease. *J Thorac Imaging* 1985;1:54–64.

25. Genereux GP. The Fleischner lecture: computed tomography of diffuse pulmonary disease. *J Thorac Imaging* 1989; 4:50–87.
26. Aberle DR, Gamsu G, Ray SC, Feurstein IM. Asbestos-related pleural and parenchymal fibrosis: detection with high-resolution CT. *Radiology* 1988;166:729–34.
27. Remy-Jardin M, Boulenguez C, Edme JL, Sobazek A, Wallaert B, Remy J. Morphologic effects of cigarette smoking on airways and pulmonary parenchyma in healthy adult volunteers: CT evaluation and correlations with pulmonary function tests. *Radiology* 1993;186:107–15.
28. Colby TV, Carrington CB. Infiltrative lung disease. In: Thurlbeck WM, ed. *Pathology of the lung*. Stuttgart, New York: Thieme, 1988.
29. Flint A. Pathologic features of interstitial lung disease. In: Shartz MI, King TE, eds. *Interstitial lung disease*. Toronto: Decker, 1988.
30. Wescott JL, Cole SR. Traction bronchiectasis in end-stage pulmonary fibrosis. *Radiology* 1986;161:665–9.
31. Grenier P, Valeyre D, Cluzel P, et al. Chronic diffuse interstitial lung disease: diagnostic value of chest radiography and high resolution CT. *Radiology* 1991;179:123–32.
32. Keogh BA, Crystal RG. Alveolitis: the key to the interstitial lung disorders. *Thorax* 1982;37:1–10.
33. Niederman MS, Matthay RA. New techniques for assessment of interstitial lung disease. *Radiol Clin North Am* 1983; 21:667–81.
34. Whitcomb ME, Dixon GF. Gallium scanning, bronchoalveolar lavage and the national debt [Editorial]. *Chest* 1984;85: 719–21.
35. Walters EH, Gardiner PV. Bronchoalveolar lavage as a research tool. *Thorax* 1991;46:613–8.
36. Helmers RA, Hunninghake GW. Bronchoalveolar lavage in the nonimmunocompromised patient. *Chest* 1989;96:1184–90.
37. Müller NL, Miller RR, Webb WR, Evans KG, Ostrow DN. Fibrosing alveolitis: CT-pathologic correlation. *Radiology* 1986;160:585–8.
38. Müller NL, Staples C, Miller RR, Vedal S, Thurlbeck WM, Ostrow DN. Disease activity in idiopathic pulmonary fibrosis: CT and pathologic correlation. *Radiology* 1987;165: 731–4.
39. Lynch DA, Webb WR, Gamsu G, et al. Computed tomography in pulmonary sarcoidosis. *J Comput Assist Tomogr* 1989;13:405–10.
40. Klein JS, Webb WR, Gamsu G, et al. Hazy increased density in diffuse lung disease: high resolution CT [Abstract]. *Radiology* 1989;173:140.
41. Noma S, Herman PG, Khan A, Chawla K. Ground-glass attenuation at high resolution CT in diffuse lung disease [Abstract]. *Radiology* 1991;181:117.
42. Hansell DM, Wells AU, Dubois R, Corrin B. Disease activity in fibrosing alveolitis: assessment by high resolution CT with histological correlation [Abstract]. *Clin Radiol* 1990;42: 375.
43. Cherniak RM, Crystal RG, Kalica AR. Current concepts in idiopathic pulmonary fibrosis: a road map for the future. NHLIB Workshop summary. *Am Rev Respir Dis* 1991;143: 680–3.
44. Vedal S, Welsch EV, Miller RR, Müller NL. Desquamative interstitial pneumonia: computed tomographic findings before and after treatment with corticosteroids. *Chest* 1988;93: 215–7.
45. Bergin CJ, Wirth RL, Berry GJ, Castellino RA. *Pneumocystis carinii* pneumonia: CT and HRCT observations. *J Comput Assist Tomogr* 1990;14:756–9.
46. Graham NJ, Müller NL, Miller RR, Shepherd JD. Intrathoracic complications following allogeneic bone marrow transplantation: CT findings. *Radiology* 1991;181:153–6.
47. Kuhlman JE, Fischman EK, Siegelman SS. Invasive pulmonary aspergillosis in acute leukemia: characteristic findings on CT, the halo sign and the role of CT in early diagnosis. *Radiology* 1985;157:611–4.
48. Noma S, Herman PG, Khan A, Rojas KA, Pipman Y. Sequential morphologic changes of elastase-induced pulmonary emphysema in pig lungs: evaluation by high resolution computed tomography. *Invest Radiol* 1991;5:446–53.
49. Rounds S, Hill NS. Pulmonary hypertensive diseases. *Chest* 1984;85:397–405.
50. Martin KW, Sagel SS, Siegel BA. Mosaic oligemia simulating pulmonary infiltrates on CT. *AJR* 1986;147:670–3.
51. Remy-Jardin M, Wattinne L, Remy J. Transcatheter occlusion of pulmonary arterial circulation and collateral supply: failures, incidents and complications. *Radiology* 1991;180: 699–705.
52. Remy J, Remy-Jardin M, Wattinne L, Deffontaines C. Pulmonary arteriovenous malformations: evaluation with CT of the chest before and after treatment. *Radiology* 1992;182: 809–15.
53. Kuriyama K, Gamsu G, Stern RG, Cann CE, Herfkens RJ, Brundage BH. CT-determined pulmonary artery diameters in predicting pulmonary hypertension. *Invest Radiol* 1984; 19:16–22.
54. Moore NR, Scott JP, Flower CDR, Higenbottam TW. The relationship between pulmonary artery pressure and pulmonary artery diameter in pulmonary hypertension. *Clin Radiol* 1988;39:486–9.
55. Grainger RG. Interstitial pulmonary edema and its radiological diagnosis: a sign of pulmonary venous and capillary hypertension. *Br J Radiol* 1958;31:201–17.
56. Hedlung LW, Vock P, Effman EL, Lischko MM, Putman CE. Hydrostatic pulmonary edema: an analysis of lung density changes by computed tomography. *Invest Radiol* 1984; 19:254–62.
57. Wegener T, Wegenius G, Hemmingsson A, Ljung B, Salldeen T. Computed chest tomography in rats with pulmonary damage due to microembolism. *Acta Radiol Diagn* 1986;27: 723–8.
58. Wegenius G. Model simulations of pulmonary edema: phantom studies with computed tomography. *Invest Radiol* 1991; 26:149–56.
59. Coates G, Powles PP, Morrison SC, Sutton JR, Webber CE, Zylak CJ. The effects of intravenous infusion of saline on lung density, lung volumes, nitrogen washout, computed tomographic scans and chest radiographs in humans. *Am Rev Respir Dis* 1983;127:91–6.
60. Remy-Jardin M, Deffontaines C, Dupont S, Gosselin B, Remy J. Les malformations congénitales de la circulation lymphatiques du thorax (lymphangiomes kystiques exceptés). *Rev Imag Med* 1990;2:733–41.
61. Maltby JD, Gouverne ML. CT findings in pulmonary venoocclusive disease. *J Comput Assist Tomogr* 1984;8:758–61.